Control of Reaction Selectivity via Surface Oxygen Coverage: Thermal Decomposition of Azomethane on Rh(111)

C. W. J. Bol, J. D. Kovacs, M. Chen, and C. M. Friend*

Department of Chemistry, Harvard University, Cambridge, Massachusetts 02138

Received: August 30, 1996; In Final Form: June 11, 1997[⊗]

The thermal decomposition of azomethane on clean and oxygen-covered Rh(111) has been investigated using a combination of temperature-programmed reaction, high-resolution electron energy loss and Fourier transform infrared spectroscopies. On clean Rh(111), azomethane adsorbs molecularly in the *trans* conformation and is stable on the surface up to 250 K. Above 300 K azomethane reacts exclusively by nitrogen−nitrogen bond scission, yielding gaseous HCN, H_2, N_2, and C_2N_2. HCN is evolved in four peaks between 300 and 600 K. Adsorbed CN reacts via two competing pathways: recombination to cyanogen and dissociation to adsorbed N, which recombines to gaseous N_2 above 600 K. Adsorbed oxygen inhibits N═N bond breaking, leading to the carbon−nitrogen bond dissociation products CO, CO_2, and formaldehyde. On Rh(111)-p(2×1)-O ($\theta_O = 0.5$ monolayers), ∼77% of the azomethane reacts via carbon−nitrogen bond scission. The C−N bond breaking is proposed to occur via adsorbed CH_2═N−N−CH_3, based on vibrational and temperature-programmed reaction data. Subsequent carbon−nitrogen bond cleavage yields gaseous N_2 and is proposed to be accompanied by formation of transient CH_2 and CH_3, which add to surface oxygen. Methyl would add to oxygen to form methoxy, which rapidly dehydrogenates to produce CO, CO_2, and H_2O. Gaseous formaldehyde is proposed to form from addition of CH_2 to oxygen followed by rapid desorption. The variation in the product distributions with oxygen coverage indicates a subtle interplay between the inhibition of nitrogen−nitrogen and C−H bond cleavage by oxygen and is cast in a general framework for hydrocarbon oxidation on Rh surfaces.

Introduction

There is an increasing interest in the chemistry of methyl and other small hydrocarbon fragments on transition metal surfaces because of their relevance to many industrial processes. For instance, the interaction of these adsorbates with oxygen is of pivotal importance in methane oxidation.[1] Pyrolysis of gaseous azomethane is frequently used as a source of methyl by cleavage of the weak carbon−nitrogen bonds to form N_2 and two $^{\bullet}CH_3$ around 500 K.[2] Accordingly, there have been several studies of azomethane on transition metal surfaces aimed at heterogeneously producing methyl; however, in all studies to date, azomethane mainly decomposes via nitrogen−nitrogen bond scission.[3−6] Carbon−nitrogen bond dissociation is only induced by electronic excitation, such as the electron-induced decomposition of azomethane on Ag(111)[7] and the ultraviolet photolysis of azomethane condensed on Pd(111).[8]

The decomposition of azomethane on Pt(111) was proposed to proceed through isomerization to *cis*-azomethane upon adsorption followed by tautomerization to formaldehyde methyl hydrazone around 200 K,[6] which yields HCN_g over the range 300−470 K in three peaks.[4] Similarly, azomethane isomerizes to the *cis* isomer upon adsorption on Mo(110) at 100 K, as shown by high-resolution electron energy loss spectroscopy.[3] As on Pt(111), the thermal decomposition of azomethane on Mo(110) was shown to proceed in part through tautomerization to formaldehyde methyl hydrazone (CH_2═NNHCH_3). The tautomerization of *cis*-azomethane to formaldehyde methyl hydrazone has also been observed in both gas-phase[9] and transition metal complex chemistry.[10]

Herein we report the thermal decomposition of azomethane on Rh(111) and the influence of surface oxygen on the decomposition pathway. On clean Rh(111) azomethane decomposes above 250 K by nitrogen−nitrogen bond scission, yielding H_2, HCN, C_2N_2, N_2, and C_a, similar to reaction on Pd(111)[5] and Pt(111).[4,6] High-resolution electron energy loss studies suggest that azomethane adsorbs molecularly on Rh(111) at 100 K in the *trans* conformation. Thermal dissociation of azomethane ultimately leads to formation of HCN and adsorbed cyanide (C≡N). The adsorbed cyanide undergoes competitive recombination to cyanogen (C_2N_2) and decomposition to adsorbed carbon and adsorbed atomic nitrogen, the latter of which recombines to form N_2 above 600 K.

Adsorbed oxygen dramatically alters the reactive chemistry of azomethane on Rh(111) such that carbon−nitrogen bond scission becomes an important pathway, ultimately dominating the reactions in the highest oxygen coverage studied, Rh(111)-p(2×1)-O ($\theta_O = 0.5$). Tautomerization followed by dehydrogenation is proposed to yield adsorbed CH_2═N═NCH_3 in which subsequent carbon−nitrogen bond cleavage leads to the formation of transient alkyl fragments, which in turn add to surface oxygen to yield gaseous formaldehyde, CO, CO_2, and H_2O. Surface oxygen similarly leads to competing C−N and N−N bond breaking on Pt(111), although N−N bond breaking remains a dominant pathway on this surface.[4] Notably, there is no production of formaldehyde on oxygen-covered Pt(111).[4] The differences in the effect of oxygen on the reactions of azomethane on Pt and Rh are mainly attributed to the differences in the ability of oxygen to form OH_a on the two surfaces, although reaction at the edges of oxygen islands may also play a role on Pt(111).[4] Oxygen on Rh(111) is known to inhibit C−H bond activation, whereas oxygen on Pt(111) readily reacts with C−H bonds to yield adsorbed hydroxyl.[11,12] Thus, these studies illustrate the important differences in the electronic properties of oxygen on transition metal surfaces in determining the product distributions in oxidation reactions.

[⊗] Abstract published in *Advance ACS Abstracts,* July 15, 1997.

S1089-5647(96)02681-8 CCC: $14.00

Experimental Section

Experiments were performed in two stainless steel vacuum chambers, both with base pressures below 1×10^{-10} Torr, described in detail elsewhere.[3,13] The preparation of the crystal,[14] the routine cleaning procedures,[14] and the preparation of the oxygen overlayers[15] have all been described previously.

In temperature-programmed reaction experiments the reactants were introduced to the clean or oxygen-covered crystal at 100 K. The crystal was then radiatively heated in line-of-sight to an apertured mass spectrometer detector (UTI-100C) to monitor gas-phase products. A wide scan of masses between 2 and 100 amu was performed using data acquisition software by Liu.[16] The crystal was negatively biased at −60 V to preclude electron-induced chemistry. For heating above 900 K, electron bombardment was used. The absolute yields of CO and CO_2 were determined by comparison of the integrated mass spectrometer signal for CO desorption from Rh(111)-(2×2)-3 CO[17−19] ($\theta_{CO} = 0.75$) and the oxidation of CO to CO_2 on Rh(111)-p(2×1)-O, respectively, as described in detail previously.[20] The yield of CH_2O is determined using the oxygen balance; the amount of oxygen left after reaction up to 800 K equals $0.5 - Y(CO) - Y(CH_2O) - 2Y(CO_2) - Y(H_2O)$, where $Y(i)$ refers to the various yields. The amount of oxygen left after reaction $Y(CO)$, and $Y(CO_2)$ are all measured quantities, while $Y(H_2O)$ can be determined by comparison to a known amount of water formation in the reaction of CH_2I_2 on Rh(111)-p(2×1)-O.[11]

In high-resolution electron energy loss and Fourier transform infrared reflection absorption experiments, the reactants were introduced to the clean or oxygen-covered surface at 100 K and the crystal was radiatively heated to the desired temperature at the same rate as used in the temperature-programmed reaction experiments. Spectra were recorded after cooling to 100 K. The electron energy loss spectrometer (LK2000-14-R) was operated at a primary beam energy of 3 eV. All spectra shown were recorded at specular detection angles. All infrared spectra were collected with a Nicolet 800 spectrometer and averaged over 500 scans at 4 cm^{-1} resolution using an MCT-A detector. Sample spectra were ratioed against a background taken immediately after the sample scan by flashing the crystal to 1000 K and scanning after the crystal had returned to 100 K.

Azomethane was synthesized from 1,2-dimethylhydrazine dichloride (Aldrich, 99%), using the procedure described by Renaud and Leitch.[21] The sample was subjected to several freeze−pump−thaw cycles before each day of experiments. The purity of the sample was regularly confirmed by mass spectrometry, which showed that no detectable decomposition occurred in the doser. Azomethane was directly dosed onto the crystal, which was positioned approximately 5 mm from the aperture of the doser. The pressure rise during dosing was typically on the order of 2×10^{-11} Torr. $^{16}O_2$ (Matheson, 99.998%) and $^{18}O_2$ (Cambridge Isotopes, 98%) were used as received.

Results

Temperature-Programmed Reaction. Azomethane decomposes exclusively by nitrogen−nitrogen bond scission, yielding H_2, HCN, C_2N_2, and N_2 during temperature-programmed reaction on clean Rh(111) (Figure 1). No other products, specifically no products of C−N bond cleavage, were detected in an extensive search between 2 and 100 amu. At high exposures, intact azomethane desorbs in two peaks around 175 and 270 K. The 175 K peak increases indefinitely with exposure and is attributed to the sublimation of condensed layers of azomethane. The 270 K peak is present even at very low exposures and is attributed to a competing desorption pathway

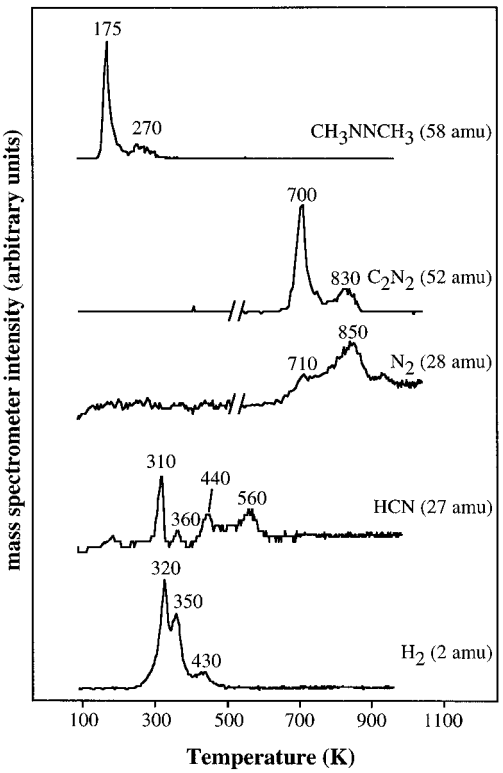

Figure 1. Temperature-programmed reaction data obtained following adsorption of azomethane on clean Rh(111). H_2, HCN, N_2, C_2N_2, and azomethane evolution is monitored at 2, 27, 28, 52, and 58 amu, respectively. The heating rate decreases monotonically from 9K/s at 100 K to 6K/s at 700 K and is highly reproducible. The high-temperature N_2 and C_2N_2 signals were collected by heating to 600 K using the heating rate of the low-temperature ramp, cooling to 255 K, and then heating to 1000 K. No other products were observed during the high-temperature ramp. The heating rate decreases monotonically from 40 K/s at 255 K to 5 K/s at 1000 K for the high-temperature ramp.

of azomethane from the monolayer. The coverage at which evolution of intact azomethane at 175 K is first observed is defined as saturation coverage. Dihydrogen evolves in a broad feature between 250 and 500 K, consisting of three overlapping peaks around 320, 350, and 430 K, while HCN is produced in four peaks at 310, 360, 440, and 560 K (Figure 1).[22] C_2N_2 evolves in two peaks at 700 and 830 K, the temperatures previously reported for recombination of adsorbed CN in the reactions of CH_3NH_2 and C_2N_2 on clean Rh(111).[23,24] N_2 desorbs in a broad peak above ∼650 K and is attributed to the recombination of adsorbed atomic nitrogen.

Surface oxygen dramatically alters the reactions of azomethane on Rh(111) such that pathways involving carbon−nitrogen bond scission are opened. Formaldehyde and dinitrogen are produced concurrently below 450 K, and H_2O, CO, and CO_2 are evolved below 600 K (Figure 2). There is no evidence for NO formation at any oxygen coverage. The selectivity for C−N over N−N bond breaking increases with increasing oxygen coverage so that C−N bond breaking is dominant at oxygen coverages approaching 0.5 monolayers (ML) (Figure 3). The yields of formaldehyde and low-temperature dinitrogen, products of C−N bond scission, increase monotonically with increasing oxygen coverage. The temperature of the formaldehyde evolution (345 K) remains unchanged with varying oxygen coverage, but the temperature of dinitrogen elimination decreases from 410 K on Rh(111)-p(2×2)-O ($\theta_O = 0.25$ ML) to 345 K on Rh(111)-p(2×1)-O ($\theta_O = 0.5$ ML) (Figure 2). The low temperature for N_2 production indicates that N_2 is eliminated directly into the gas phase from a single azomethane molecule, since molecular

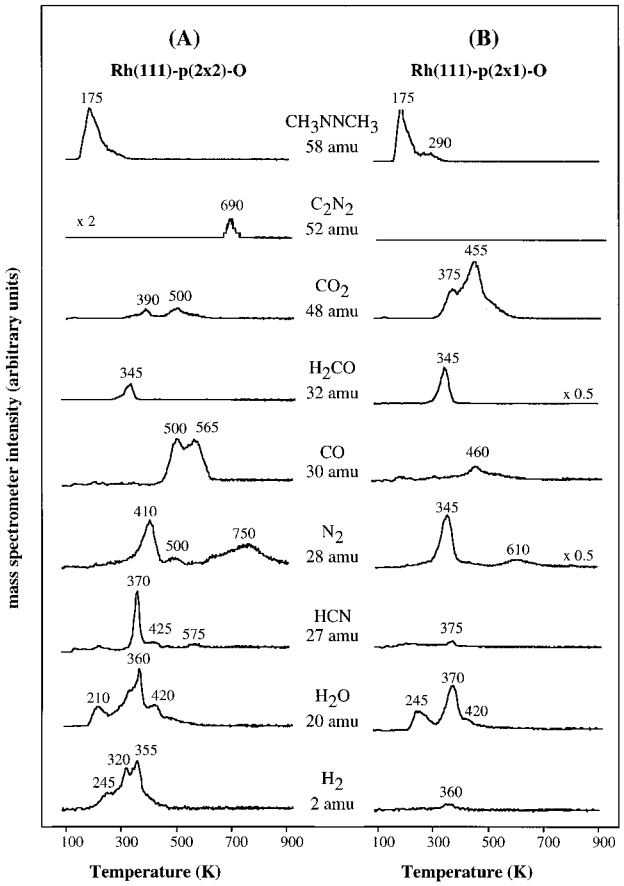

Figure 2. Temperature-programmed reaction of azomethane on (A) Rh(111)-p(2×2)-^{18}O and (B) Rh(111)-p(2×1)-^{18}O. H_2, $H_2{}^{18}O$, HCN, N_2, CO, $H_2C^{18}O$, $C^{18}O_2$, C_2N_2, and azomethane evolution is monitored at 2, 20, 27, 28, 30, 32, 48, 52, and 58 amu, respectively. All signals are corrected for contributions from fragmentation of other products. The heating decreases monotonically from 9 K/s at 100 K to 6 K/s at 700 K and is highly reproducible.

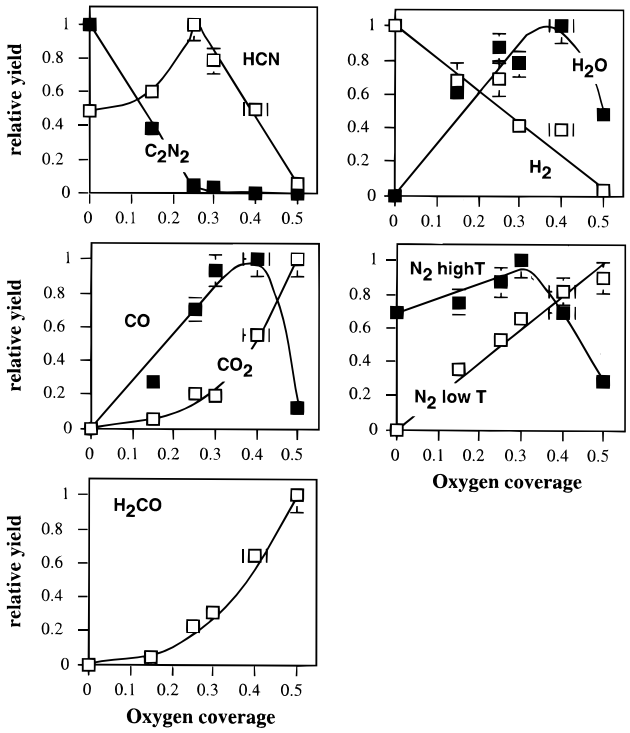

Figure 3. Variation of product yields in temperature-programmed reaction as a function of initial oxygen coverage. The yields are determined from the integrated intensity vs temperature profiles using the masses shown in Figures 1 and 2. The high-temperature N_2 corresponds to nitrogen recombination, the area above 600 K, whereas low-temperature N_2 is molecular desorption, corresponding to the integrated yield below 600 K. All oxygen-containing products are ^{18}O-substituted. All signals have been corrected for contributions from fragmentation of other products. Yields are normalized to the maximum mass spectrometer signal observed for a particular product.

nitrogen desorbs at ∼140 K from Rh(111) and nitrogen atom recombination occurs above 600 K.

Although the combined yields of products from N−N bond scission monotonically decrease with increasing oxygen coverages, production of both HCN and recombinative N_2 first increases and later decreases with increasing oxygen coverage. On Rh(111)-p(2×2)-O ($\theta_O = 0.25$) the yield of HCN[22] is at a maximum, evolving in a large peak at 370 K and two smaller ones at 425 and 575 K. Only a trace amount of HCN evolves at 375 K from Rh(111)-p(2×1)-O (Figure 2). The amount of recombinative (high-temperature) N_2 reaches a maximum at an oxygen coverage of 0.3 monolayers (Figure 3). The peak temperature for nitrogen recombination decreases to 610 K on Rh(111)-p(2×1)-O compared to 850 K on clean Rh(111) (Figures 1 and 2). The yield of C_2N_2 monotonically and sharply decreases with increasing oxygen coverage such that no more C_2N_2 is detected above an oxygen coverage of 0.4 ML. The temperature of C_2N_2 evolution is essentially constant, around 700 K.

The combined yields of H_2 and H_2O show that dehydrogenation is inhibited by oxygen on Rh(111). The yield of dihydrogen falls monotonically with increasing oxygen coverage to virtually zero on Rh(111)-p(2×1)-O ($\theta_O = 0.5$ monolayers). On Rh(111)-p(2×2)-O, H_2 is evolved in three peaks at 245, 320, and 355 K; on Rh(111)-p(2×1)-O only a small peak at 360 K remains (Figure 2). The yield of H_2O, the other dehydrogenation product, initially rises and later falls as a function of increasing oxygen coverage, reaching a maximum for 0.4 monolayers of oxygen (Figure 3). Water evolves at 245 and 370 K with a shoulder at 420 K on Rh(111)-p(2×1)-O (Figure 2). Hence, the total amount of dehydrogenation diminishes as the initial oxygen coverage is raised above 0.4 ML. Note that the formation of H_2O at low temperature removes oxygen and thus opens some Rh sites. The increase in formaldehyde production is attributed to the inhibition of dehydrogenation by oxygen. A similar inhibition of nonselective dehydrogenation by oxygen has been observed in the reactions of olefins[25−27] and alkyl iodides[20] on Rh(111).

The yields of CO and CO_2 both initially increase as a function of oxygen coverage. However, CO formation dramatically declines for oxygen coverages above 0.4 monolayers (Figure 3). Over the same oxygen coverage range, the yield of CO_2 increases. The increase in CO_2 over CO production is attributed to an enhanced rate of CO oxidation at higher oxygen coverages. The temperatures of CO and CO_2 evolution decrease slightly as the oxygen coverage is increased from the p(2×2)-O to the p(2×1)-O overlayer, from 500 and 565 K to 460 K for CO, and from 390 and 500 K to 375 and 455 K for CO_2 (Figure 2).

On Rh(111)-p(2×1)-O, an estimated 0.091 ± 0.018 molecules of azomethane react per surface rhodium atom, based on the carbon balance. The total amount of azomethane reaction equals half of the sum of the yields of CO, CO_2, and CH_2O, the only carbon-containing products on Rh(111)-p(2×1)-O.[28] Of the azomethane that reacts, 77% decomposes via C−N bond scission, based on the yield of low-temperature dinitrogen relative to the yield of the recombination of atomic nitrogen at higher temperatures. Based on the integrated mass spectrometer signal intensity in the water evolution at 245 K, ∼97% of the azomethane has lost one hydrogen at this temperature.[29] The saturation coverage of azomethane on clean Rh(111) cannot be

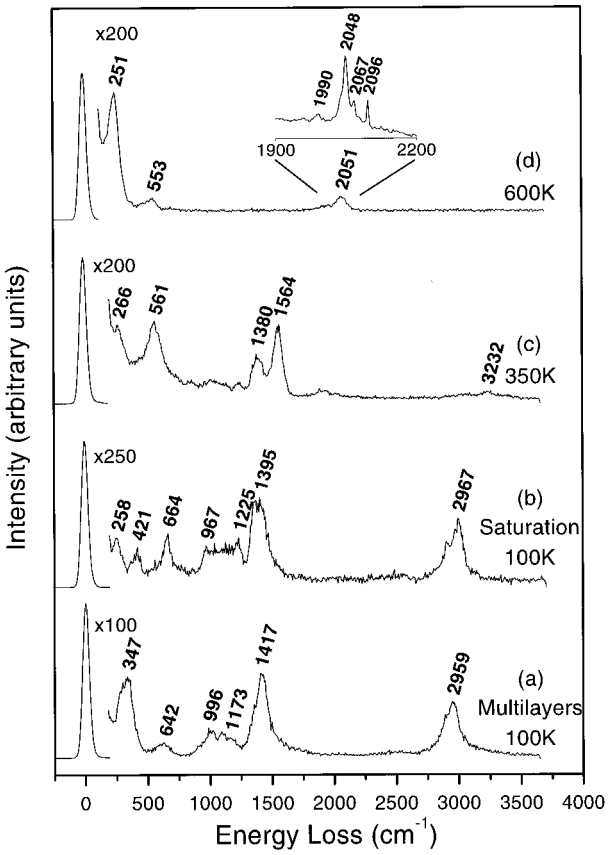

Figure 4. High-resolution electron energy loss spectra of azomethane on clean Rh(111) showing (a) multilayers after adsorption at 100 K and saturation coverage (b) after adsorption at 100 K, (c) after annealing to 350 K, and (d) annealing to 600 K. The full widths at half maximum (fwhm) of these spectra are approximately 60 cm^{-1}. Inset above (d) shows the Fourier transform infrared spectrum of a saturation coverage of azomethane annealed to 600 K. The resolution of the infrared spectrum is 4 cm^{-1}.

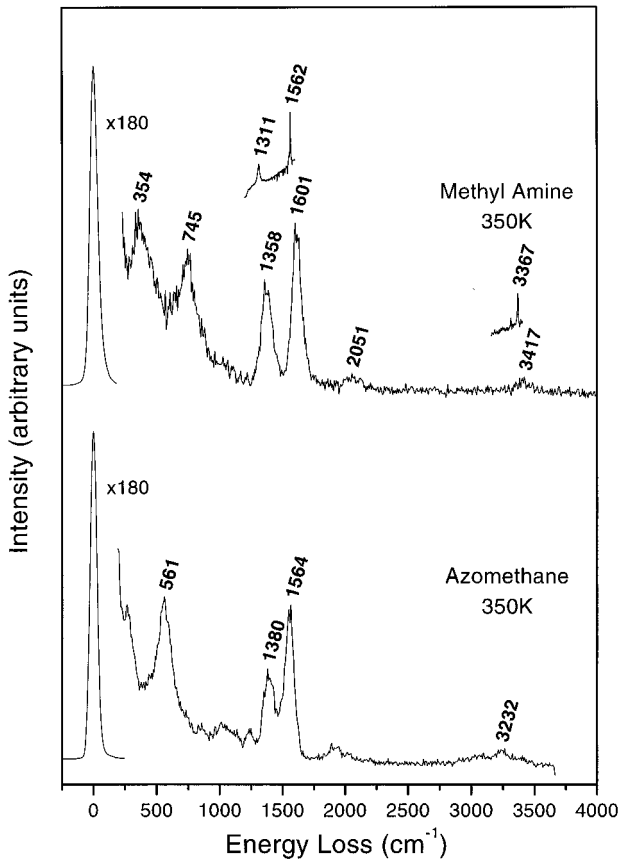

Figure 5. High-resolution electron energy loss spectra of azomethane on clean Rh(111) heated to 350 K (bottom) and methylamine on clean Rh(111) heated to 350 K (top). The corresponding infrared data for methylamine on clean Rh(111) heated to 350 K are shown as an inset at the top for comparison to the modes of aminomethylidyne on Pt(111). The full widths at half maximum (fwhm) of the electron energy loss spectra are 72 cm^{-1} for methylamine and 63 cm^{-1} for azomethane. The resolution of the infrared spectrum is 4 cm^{-1}.

quantitatively determined because of the multiplicity of products that do not have known coverages.

Vibrational Studies. Vibrational data obtained following a saturation dose of azomethane on clean Rh(111) at 100 K are consistent with intact *trans*-azomethane based on correspondence to the spectrum of the multilayer, to azomethane on other surfaces,[3,6] and to condensed azomethane[30,31] (parts a and b of Figure 4). The monolayer and multilayer spectra are essentially identical except for a redistribution of peak intensities between 1000 and 1200 cm^{-1} in the electron energy loss data (Figure 4). The spectrum remains essentially unchanged up to 250 K, indicating persistence of intact *trans*-azomethane. The assignment of the spectrum in terms of intact azomethane is consistent with the observed desorption of the intact molecule at 270 K. The relatively low intensity around 1090 cm^{-1} is evidence that the *trans* form predominates over *cis*-azomethane on Rh(111). *cis*-Azomethane has been previously identified on Mo(110) on the basis of an intense mode at 1090 cm^{-1}.[3]

There is no evidence for low-temperature dehydrogenation reactions in the vibrational data obtained at 100 K. Notably, there is no indication of a C═N bond or sp^2 carbon in the spectrum, which would be signified by peaks near 3100 cm^{-1} (asymmetric CH_2 stretch) and 800 cm^{-1} (CH_2 wag). A C═N stretch might also be observed between 1200 and 1600 cm^{-1}. (The corresponding modes from formaldehyde dimethyl hydrazone occur at 3084 and 784 cm^{-1}.[32]) Furthermore, there is no evidence for N−H bond formation. There is no intensity near 3200 cm^{-1}, the N−H stretch region, or in the regions expected for the NH_2 wag of CH_3NH_2 (∼750 cm^{-1})[33] or the δ(N−H) of an RNH group (∼900 cm^{-1}).[6]

Furthermore, there is no evidence for a significant amount N═N bond cleavage at low temperatures to form methylimido (CH_3N). In organometallic compounds containing a NCH_3 group, a strong C−N stretch is observed between 1020 and 1100 cm^{-1} [34] that is not present in the electron energy loss spectrum of azomethane on clean Rh(111). The C−N stretch would be expected to have a strong dipole component along the surface normal analogous to that of methoxy, for which the intensity of the C−O stretch is over 5 times stronger than the intensity of the methyl deformation on Rh(111).[35] Therefore, if CH_3N were present in significant amounts, a strong C−N stretch should be detected in both electron energy loss and infrared spectra. Instead, there is only a relatively weak and unresolved band in the electron energy loss spectrum in this region (Figure 4b).

Azomethane decomposition occurs over the range 250−350 K, as signified by changes in the vibrational spectrum (Figure 4) as well as the onset of H_2 evolution during temperature-programmed reaction (Figure 1). Although a definitive assignment of the intermediates present on the rhodium surface over this range is not possible, aminomethylidyne, which has been identified as the major intermediate of azomethane decomposition on Pt(111),[6] can be ruled out based on vibrational data. Aminomethylidyne (CNH_2) can be independently synthesized on Rh(111) by heating methylamine to 350 K and is unequivocally identified based on comparison of the infrared spectrum to that of aminomethylidyne on Pt(111).[36] The modes in the infrared spectrum on Rh(111) at 3367, 1562, and 1311 cm^{-1} are assigned to the ν(N−H), $\delta(NH_2)$, and ν(CN), respectively (Figure 5, inset). The corresponding peaks in the electron

energy loss spectrum are 3417 cm^{-1} (ν(N−H)), 1601 cm^{-1} ($\delta(NH_2)$) and 1358 cm^{-1} (ν(CN)) (Figure 5). The mode at 745 cm^{-1} is assigned to the Rh−CN deformation and 354 cm^{-1} to the M−CNH_2 stretch based on a normal mode analysis of aminomethylidyne on Pt(111) by Jentz et al.[37] The lack of intensity at 354, 745, and 3417 cm^{-1} in the electron energy loss spectrum of azomethane heated to 350 K (Figure 5, bottom) clearly indicates that the dominant species derived from azomethane on the surface is *not* aminomethylidyne.

Vibrational data are consistent with the presence of various forms of HCN after heating to 350 K, although other intermediates are probably also present based on the fact that H_2 evolution has already commenced. The frequency of 3232 cm^{-1} is consistent with the presence of N-bound HCN, based on comparison with the ν(C−H) of 3298 cm^{-1} for N-bound HCN on Pt(111).[36] Although the ν(C≡N) was not reported for N-bound HCN on Pt(111), the peak at 2040 cm^{-1} is similar to the experimental gas-phase value (2097 cm^{-1})[38] and the calculated value of 2200 cm^{-1} for HCN bound to the fcc 3-fold site on Ni(111).[39] Side-bound HNC is another possible intermediate giving rise to some of the vibrational peaks obtained after heating to 350 K. The frequency of 1564 cm^{-1} is similar to the ν(CN) energy calculated for HNC oriented parallel to Ni(111), 1530 cm^{-1},[39] for example, and analogous N−H bond formation has previously been observed on Pt(111)[36] and W(100)-(5×1)-C,[40,41] as well as in organometallic complexes.[42] The assignment of modes in terms of HCN is also consistent with the observation of HCN evolution in this temperature range and above. However, the assignments are not unique.

At 600 K, only adsorbed CN remains on the surface as identified by ν(C≡N) at 2051 cm^{-1} and ν(Rh−CN) at 251 cm^{-1} in the electron energy loss spectrum (Figure 4d). The peak at 560 cm^{-1} is assigned to a convolution of the Rh−N and Rh−C stretches of adsorbed atomic nitrogen and carbon from the decomposition of adsorbed CN. The relatively high frequency of the carbon−nitrogen stretch indicates a bond order of approximately 3. Although only two peaks, at 1850 and 2051 cm^{-1}, are resolved in electron energy loss, there are at least four well-resolved peaks in this region in the infrared spectrum (Figure 4d, inset). The intensities of these peaks are very reproducible at a given temperature and dose but redistribute and shift depending on the annealing temperature. A detailed analysis is not possible without isotopic labeling and coverage-dependent experiments. However, the multiplicity of peaks indicates a heterogeneity in bonding environments of the adsorbed CN. A similar behavior pattern was observed after heating methylamine to 450 K on Rh(111) (data not shown), indicating that this is not specific to the decomposition of azomethane.

Vibrational studies of azomethane adsorbed on Rh(111)-p(2×1)-O are consistent with results from temperature-programmed reaction spectroscopy, which indicate that N−N bond dissociation does not occur to a significant degree at any temperature. The presence of the ν(N═N) stretch at 1572 cm^{-1} clearly indicates that the N═N bond is retained on Rh(111)-p(2×1)-O at 100 K and this spectrum can be readily assigned to intact *trans*-azomethane (Figure 6b). The ν(N═N) is also observed in the infrared spectrum (not shown); thus, the vibration must be dipole-scattered and have a significant dipole moment perpendicular to the surface plane. Furthermore, the presence of the ν(CN) (1005 cm^{-1}) and the strong ν(CH) at 2916 cm^{-1} in the infrared spectra on Rh(111) (data not shown) is evidence that the azomethane adsorbs in the *trans* conformation with C_s symmetry (i.e., with the N═N axis tilted away from the surface), based on a symmetry analysis by Jentz and co-workers.[6] The spectrum remains unchanged after heating to 200 K, suggesting that azomethane remains intact up to this temperature. The strong mode at 553 cm^{-1} is assigned primarily to the ν(Rh−O) of adsorbed atomic oxygen based on the comparison to the as-prepared Rh(111)-p(2×1)-O surface for which there is a single mode at ∼560 cm^{-1}. There may also be a contribution from the δ(CNN) mode, which is observed at 584 cm^{-1} for solid *trans*-azomethane.[31]

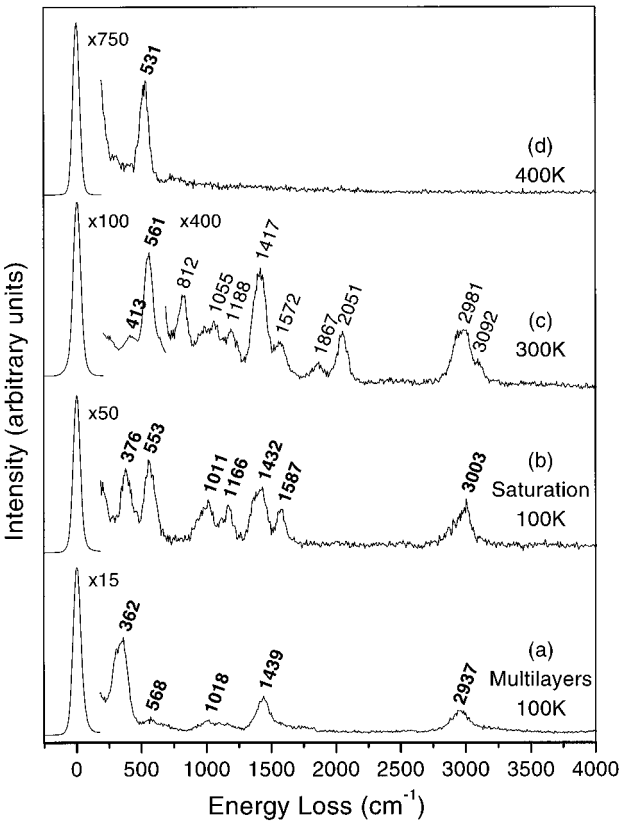

Figure 6. High-resolution electron energy loss spectra of azomethane on Rh(111)-p(2×1)-^{16}O showing (a) multilayers after adsorption at 100 K and saturation coverage (b) after adsorption at 100 K, (c) after annealing to 300 K, and (d) after annealing to 400 K. The full widths at half maximum (fwhm) of these spectra are 71, 64, 68, and 59 cm^{-1}, respectively.

Azomethane reacts between 200 and 300 K, and a surface-bound CH_2N−NCH_3 species is proposed to form, based on a combination of temperature-programmed reaction and vibrational data (Figure 6). A reasonable pathway for CH_2N−NCH_3 formation is tautomerization of azomethane to formaldehyde methyl hydrazone (CH_2═N−NH−CH_3) and subsequent cleavage of the relatively weak N−H bond. Half an equivalent of H_2O is formed per azomethane at 245 K during temperature-programmed reaction, leading support for this argument and ruling out an assignment in terms of intact azomethane (Figure 2). Tautomerization of azomethane to formaldehyde methyl hydrazone occurs on Mo(110)[3] and on Pt(111)[6] as well as in transition metal complexes.[10] However, the absence of a ν(N−H) mode near 3300 cm^{-1} [3] indicates that, if formed, the N−H bond is cleaved on Rh(111)-p(2×1)-O. All the modes in the spectrum collected after heating a saturation coverage of azomethane on Rh(111)-p(2×1)-O to 300 K can be assigned to CH_2═N−NCH_3 and atomic oxygen on the surface, based on comparison to the spectra of formaldehyde methyl hydrazone adsorbed on Pt(111)[6] and on Mo(110)[3] and on infrared and Raman data of formaldehyde dimethyl hydrazone.[32,43] In particular, the high-frequency shoulder in the C−H stretch region at 3092 cm^{-1} along with the CH_2 twist at 812 cm^{-1} indicates that there is sp^2 carbon present. The analogous modes

are at 3084 and 784 cm^{-1} in gaseous formaldehyde dimethyl hydrazone.[32] The set of unresolved peaks between 1000 and 1100 cm^{-1} is ascribed to a convolution of $\rho(CH_3)$ and $\rho(CH_2)$ modes, whereas the peak at 1188 cm^{-1} is assigned to the ν(N−N) mode, based on assignments for Pt(111).[6] The peak at 1572 cm^{-1} is tentatively assigned to the ν(C═N) mode, based on the similar frequency of this mode for gas-phase formaldehyde dimethyl hydrazone (1586 cm^{-1}),[32] although it could also have a contribution from an N═N bond. Finally, the peak at 1417 cm^{-1} is assigned to a $\delta(CH_3)$ mode, the loss at 413 cm^{-1} to a metal−molecule stretch, and the strong loss at 560 cm^{-1} to the characteristic ν(Rh−O) mode of the atomic oxygen. The peaks at 1867 and 2051 cm^{-1} are assigned to ν(CO), not ν(CN), since both peaks disappear after heating through the temperature range where CO and CO_2 are evolved. Dehydrogenation in conjunction with C−N bond breaking occurs upon heating above 300 K. After heating to 400 K, past the temperature of carbon−nitrogen bond scission, only a mode at 531 cm^{-1} is present, which is assigned to a convolution of the stretches of atomic oxygen and atomic nitrogen.

Discussion

The products of azomethane reaction on clean Rh(111) are qualitatively similar to those on Pt(111)[4,6] and on Pd(111)[5] in that N−N bond dissociation predominates. In all three cases HCN and cyanogen are the primary products; however, gaseous methylamine is also produced on Pt(111). The lack of methylamine production from azomethane on Rh(111) is not surprising, since previous work showed that methylamine quantitatively and irreversibly decomposes to cyanogen, N_2, and HCN.[23]

The mechanism proposed for azomethane reaction on clean Rh(111), however, is different from that suggested for Pt(111).[6] Azomethane adsorbs in the *trans* conformation on Rh(111), whereas on Pt(111) it adopts the *cis* conformation. On Pt(111) isomerization of azomethane to formaldehyde methyl hydrazone was proposed to occur below 200 K followed by N−N bond cleavage to finally yield gaseous HCN and adsorbed CNH_2.[6] On Rh(111) there is no evidence for N−H bond formation at low temperature, and the vibrational spectrum cannot be assigned in terms of adsorbed CNH_2 (the intermediate identified on Pt(111)[6]) at any temperature.

As the temperature is increased above 250 K, azomethane decomposes on Rh(111) via a complex set of steps to ultimately yield adsorbed CN along with gaseous H_2 and HCN. The evolution of HCN in four discernible peaks between 275 and 600 K on Rh(111) suggests that desorption competes with dehydrogenation in several distinct processes, but the complexity of the chemistry precludes a detailed mechanistic understanding. Although gaseous HCN is also produced from reaction on Pt(111), it is derived from adsorbed CNH_2, which is clearly not a major intermediate on Rh(111). Since CNH_2 readily forms from CH_3NH_2 on Rh(111), the difference in the decomposition of azomethane on Pt versus Rh is *not* due to an intrinsic instability of aminomethylidyne. Rather, the difference must be due to differences in the most favorable reaction pathways for azomethane on the two surfaces.

Surface oxygen has a pronounced effect on the mechanism of azomethane decomposition on Rh(111), inhibiting N═N bond scission in favor of C−N bond activation. The selectivity for C−N bond scission increases with increasing oxygen coverage, based on the increase in the yield of low-temperature dinitrogen and the decrease in the yield of HCN, cyanogen, and high-temperature dinitrogen. The change in selectivity is attributed in part to the inhibition of C−H bond breaking by oxygen but may also result from a change in the bonding of azomethane to the surface. Oxygen, which occupies the 3-fold sites,[44] both geometrically blocks the surface and also modifies the local electronic structure of nearby Rh atoms.

We propose that azomethane reacts to form adsorbed CH_2═N−N−CH_3 between 200 and 300 K on Rh(111)-p(2×1)-O. The vibrational spectrum is completely consistent with the presence of CH_2═N−N−CH_3, and the amount of water evolved in the peak at 245 K indicates that one hydrogen is lost per azomethane molecule that reacts. Furthermore, both vibrational and temperature-programmed reaction data indicate that the N−N bond is retained up to 300 K. Carbon−nitrogen bond scission is signified by the formation of N_2 at 345 K and is proposed to be accompanied by formation of transient CH_3 and CH_2. Both CH_2 and CH_3 are expected to add rapidly to surface oxygen, forming gaseous formaldehyde and a short-lived methoxy intermediate, respectively. The formation of gaseous formaldehyde by direct addition of CH_2 to surface oxygen on Rh(111) has previously been observed in the reaction of CH_2I_2.[11,45] Furthermore, the identical leading edge in the evolution of dinitrogen and formaldehyde on Rh(111)-p(2×1)-O suggests that both products are formed from the same intermediate with the same rate-determining step, proposed to be dissociation of the carbon−nitrogen bonds in adsorbed CH_2═N−N−CH_3. Methyl is also known to readily add to surface oxygen to form methoxy on Rh(111)-p(2×1)-O at 100 K.[46] The methoxy formed at 345 K is expected to react immediately to form CO, CO_2, and H_2O, based on previous studies of CH_3O_a on oxygen-covered Rh(111),[35,46,47] as is observed in the azomethane reaction.

Although the amount of N−N bond retention increases nearly linearly with oxygen coverage (Figure 3), there is still a small amount of nitrogen−nitrogen bond scission even on the p(2×1)-O surface. We attribute to residual N−N bond breaking to the removal of oxygen as water around 245 K; hence, rhodium sites on the surface become accessible, and nitrogen−nitrogen bond scission occurs. We have already demonstrated a similar effect in the reaction of 2-propyl thiolate on oxygen-covered Rh(111).[15] In fact, the dependence in the product distributions on initial oxygen coverage substantiates this proposal.

A combination of C−N and N−N bond scission is induced by Rh(111) when azomethane reacts at intermediate oxygen coverages. The production of low-temperature N_2 (410 K) and H_2C═O (345 K) signify C−N bond breaking, while the evolution of C_2N_2 (690 K) and HCN (370 K) involve N−N bond dissociation in the reactions of azomethane on Rh(111)-p(2×2)-O (θ_O = 0.25 monolayers) (Figure 2). Temperature-programmed reaction of azomethane on Rh(111)-(2×2)-O largely resembles a convolution of the reactions on clean Rh(111) and Rh(111)-p(2×1)-O. The temperature range for low-temperature N_2 overlaps with the main HCN peak at 370 K on Rh(111)-(2×2)-O, suggesting that C−N and N−N bond breaking compete over this range. There is also an increase in the CO_2:CO and high-temperature N_2:C_2N_2 ratios with increasing oxygen coverage. The increase in CO_2 relative to CO is mainly attributed to an enhancement in CO oxidation at high oxygen coverages. The decrease in the yield of cyanogen relative to high-temperature N_2 is attributed to reaction of adsorbed CN with surface oxygen. Cyanide oxidation leads to CO and CO_2 production in conjunction with N_a; the nitrogen atoms subsequently recombine at high temperature.[24]

The effect of adsorbed oxygen on the reactivity of azomethane is substantially different on Rh(111) than on Pt(111);[4] the effect of oxygen on azomethane reaction was not investigated on Pd(111). On Pt(111) N−N and C−N bond breaking compete for oxygen coverages of about 0.17−0.20 monolayers on Pt(111), based on temperature-programmed reaction data.[4] Although HCN and N_2 are produced around 300 K on both

oxygen-covered Pt(111) ($\theta_O \approx 0.20$ ML) and Rh(111)-p(2×2)-O ($\theta_O = 0.25$ ML), there is no production of formaldehyde on oxygen-covered Pt(111), and instead, small amounts of methylamine and NO are formed. Furthermore, there is substantially more water formed below 300 K on oxygen-covered Pt(111) than on Rh(111)-p(2×2)-O but less H_2. The lack of NO formation in the Rh case is not surprising, since adsorbed nitrogen and oxygen do not react to form NO on Rh(111)[48] and because the O−Rh bond is considerably stronger than the O−Pt bond−85 kcal/mol for Rh[49] versus 48 kcal/mol for Pt.[50]

The differences in the reactivity of oxygen-covered Pt(111) and Rh(111) are mainly attributed to the difference in the ability of oxygen to react with C−H bonds on the two different surfaces. Oxygen on Pt readily reacts with hydrogen to produce OH_a, whereas oxygen on Rh(111) inhibits C−H bond activation. For example, dehydrogenation of cyclohexane is promoted by oxygen on Pt(111),[12] while in contrast carbon−hydrogen bond activation in olefins,[25] alkyl iodides,[11,20] and alkyl thiols[15] is inhibited by oxygen on Rh(111), and OH_a has never been observed on Rh(111) in vibrational spectroscopy. Accordingly, more hydrogen is abstracted by oxygen on Pt, thus favoring oxidation to products without C−H bonds, i.e., CO and CO_2. Although oxidation at the edges of oxygen islands was invoked in the case of Pt(111),[4] this does not explain the differences in the product distributions on Pt versus Rh; in particular, formaldehyde is not formed on Pt(111) but is formed on Rh(111) for similar oxygen coverages.

Conclusion

Azomethane decomposes exclusively via nitrogen−nitrogen bond scission on clean Rh(111), leading to the formation of gaseous HCN, C_2N_2, H_2, recombinative N_2, and surface carbon, similar to the chemistry previously observed for azomethane on Pd(111) and Pt(111). The nitrogen−nitrogen bond is cleaved upon heating above 250 K, and successive decomposition via a complex mechanism leads to the observed products.

On Rh(111)-p(2×1)-O azomethane adsorbs intact at 100 K but subsequently forms adsorbed $CH_2{=}N{-}N{-}CH_3$ via a proposed mechanism involving tautomerization followed by rapid dehydrogenation and loss of H_2O_g. Carbon−nitrogen bond scission in this intermediate leads to the formation of gaseous N_2 and transient CH_2 and CH_3. Methylene and methyl add directly to surface oxygen, forming gaseous formaldehyde and transient methoxy, respectively. Methoxy immediately dehydrogenates to CO, CO_2, and water. The formation of gaseous formaldehyde by the addition of transient CH_2 to surface oxygen is similar to chemistry previously reported for the reaction of CH_2I_2 on oxygen-covered Rh(111).

Oxygen influences the chemistry of azomethane on Rh(111) in four distinct ways. First, oxygen scavenges surface hydrogen and removes it as water. Second, oxygen blocks surface sites necessary for nitrogen−nitrogen bond scission in azomethane at low temperature. Third, oxygen inhibits nonselective C−H bond cleavage by the surface. Finally, oxygen adds directly to gaseous alkyl fragments to yield the observed products.

Acknowledgment. We gratefully acknowledge the support of the National Science Foundation under Grant No. CHE-9421615. We also thank Ms. Shira Fischer for her assistance in preparing the figures.

References and Notes

(1) Hickman, D. A.; Schmidt, L. D. *AIChE J.* **1993**, *39*, 1164−1177.
(2) Ramsperger, H. C. *J. Am. Chem. Soc.* **1927**, *49*, 912−916.
(3) Weldon, M. K.; Friend, C. M. *Surf. Sci.* **1994**, *310*, 95−102.
(4) Berlowitz, P.; Yang, B. L.; Butt, J. B.; Kung, H. H. *Surf. Sci.* **1986**, *171*, 69−82.
(5) Hanley, L.; Guo, X.; Yates, J. T. J. *J. Phys. Chem.* **1989**, *93*, 6754−6757.
(6) Jentz, D.; Trenary, M.; Peng, X. D.; Stair, P. *Surf. Sci.* **1995**, *341*, 282−294.
(7) Castro, M. E.; Pressley, L. A.; White, J. M. *Surf. Sci.* **1991**, *256*, 227−241.
(8) Hanley, L.; Guo, X.; Yates, J. T. J. *Surf. Sci.* **1990**, *232*, 129−137.
(9) Hutton, R. F.; Steel, C. *J. Am. Chem. Soc.* **1964**, *86*, 745−746.
(10) Ackermann, M. N.; Dobmeyer, D. J.; Hardy, L. C. *J. Organomet. Chem.* **1979**, *182*, 561.
(11) Bol, C. W. J.; Friend, C. M. *J. Am. Chem. Soc.* **1995**, *117*, 11572−11579.
(12) Smith, C. E.; Biberian, J. P.; Somorjai, G. A. *J. Catal.* **1979**, *57*, 426−443.
(13) Wiegand, B. C. Model Studies of Desulfurization Reactions on Mo(110). Ph.D. Thesis, Harvard University, Cambridge, MA, 1991.
(14) Xu, X.; Friend, C. M. *J. Phys. Chem.* **1989**, *93*, 8072−8080.
(15) Bol, C. W. J.; Friend, C. M. *J. Am. Chem. Soc.* **1995**, *117*, 5351−5358.
(16) Liu, A. C.; Friend, C. M. *Rev. Sci. Instrum.* **1986**, *57*, 1519−1522.
(17) Thiel, P. A.; Williams, E. D.; Yates, J. T. J.; Weinberg, W. H. *Surf. Sci.* **1979**, *84*, 54−64.
(18) Van Hove, M. A.; Koestner, R. J.; Frost, J. C.; Somorjai, G. A. *Surf. Sci.* **1983**, *129*, 482−506.
(19) Van Hove, M. A.; Koestner, R. J.; Somorjai, G. A. *Phys. Rev. Lett.* **1983**, *50*, 903−906.
(20) Bol, C. W. J.; Friend, C. M. *J. Phys. Chem.* **1995**, *99*, 11930−11936.
(21) Renaud, R.; Leitch, L. C. *Can. J. Chem.* **1993**, *32*, 545.
(22) HCN and HNC cannot be distinguished on the basis of mass spectrometer signal intensity distributions. The product is assumed to be HCN based on its greater thermodynamic stability.
(23) Hwang, S. Y.; Kong, A. C. F.; Schmidt, L. D. *J. Phys. Chem.* **1989**, *93*, 8327−8333.
(24) Solymosi, F.; Bugyi, L. *Surf. Sci.* **1984**, *147*, 685−701.
(25) Xu, X.; Friend, C. M. *J. Am. Chem. Soc.* **1991**, *113*, 6779−6785.
(26) Xu, X.; Friend, C. M. *J. Phys. Chem.* **1991**, *95*, 10753−10759.
(27) Xu, X.; Friend, C. M. *J. Am. Chem. Soc.* **1990**, *112*, 4571−4573.
(28) The trace amount of HCN production on Rh(111)-p(2×1)-O was neglected for the purposes of this calculation.
(29) The standard deviation in the measurement of the integrated mass spectrometer signal intensity for water, and consequently azomethane reaction, is 29%. Although the experimental value is highly reproducible, the quoted error is relatively large because of propagation of errors in calculations.
(30) Ackermann, M. N.; Craig, N. C.; Isberg, R. R.; Lauter, D. M.; Tacy, E. P. *J. Phys. Chem.* **1979**, *83*, 1190−1200.
(31) Durig, J. R.; Pate, C. B.; Harris, W. C. *J. Chem. Phys.* **1972**, *56*, 5652−5662.
(32) Harris, W. G.; Glenn, F. L.; Knight, L. B. Spectrochim. *Acta* **1975**, *31A*, 11−22.
(33) Baca, A. G.; Schulz, M. A.; Shirley, D. A. *J. Chem. Phys.* **1985**, *83*, 6001−6008.
(34) Schumann, H.; Schumann-Ruidisch, I.; Ronecker, S. *Z. Naturforsch.* **1970**, *25*, 565−568.
(35) Houtman, C.; Barteau, M. A. *Langmuir* **1990**, *6*, 1558−1566.
(36) Jentz, D.; Celio, H.; Mills, P.; Trenary, M. *Surf. Sci.* **1995**, *34*, 1−8.
(37) Patrick Mills, David Jentz, and Michael Trenary. Private communication.
(38) Hyde, G. E.; Hornig, D. F. *J. Chem. Phys.* **1952**, *20*, 647.
(39) Yang, H.; Whitten, J. L. *J. Phys. Chem.* **1996**, *100*, 5090−5097.
(40) Serafin, J. G.; Friend, C. M. *J. Phys. Chem.* **1988**, *92*, 6694−6700.
(41) Friend, C. M.; Serafin, J. G. *J. Chem. Phys.* **1988**, *88*, 4037−4045.
(42) Andrews, M. A.; van Buskirk, G.; Knobler, C. B.; Kaesz, H. D. *J. Am. Chem. Soc.* **1979**, *101*, 7245−7254.
(43) Wiley, R. H.; Slaymaker, S. C.; Kraus, H. *J. Org. Chem.* **1957**, *22*, 204−207.
(44) Wong, K. C.; Liu, W.; Mitchell, K. A. R. *Surf. Sci.* **1996**, *360*, 137−143.
(45) Solymosi, F.; Klivenyi, G. *J. Phys. Chem.* **1995**, *99*, 8950−8953.
(46) Bol, C. W. J.; Friend, C. M. *J. Am. Chem. Soc.* **1995**, *117*, 8053−8054.
(47) Solymosi, F.; Tarnoczi, T. I.; Berko, A. *J. Phys. Chem.* **1984**, *88*, 6170−6174.
(48) Root, T. W.; Schmidt, L. D.; Fisher, G. B. *Surf. Sci.* **1983**, *134*, 30−45.
(49) Thiel, P. A.; Yates, J. T., Jr.; Weinberg, W. H. *Surf. Sci.* **1979**, *82*, 22−44.
(50) Winkler, A.; Guo, X.; Siddiqui, H. R.; Hagans, P. L.; Yates, J. T. J. *Surf. Sci.* **1988**, *201*, 419−443.